

R-matrix theory for magnetotransport properties in semiconductor devices

Thushari Jayasekera, Michael A. Morrison, and Kieran Mullen*

Department of Physics and Astronomy, The University of Oklahoma, 440 West Brooks Street, Norman, Oklahoma 73019-0225, USA

(Received 6 August 2006; published 6 December 2006)

Many problems in nano and molecular electronics require the solution of the Schrodinger equation for scattering states. R -matrix theory, a technique first introduced in nuclear physics and widely used in atomic and molecular physics, has recently been adapted to calculate the transport properties of solid-state devices. We have extended R -matrix theory to the general case of two-dimensional devices in the presence of an external perpendicular magnetic field. We apply this technique to a particular device and calculate the magnetotransport properties of a two-dimensional “cross” junction.

DOI: [10.1103/PhysRevB.74.235308](https://doi.org/10.1103/PhysRevB.74.235308)

PACS number(s): 73.43.Qt, 73.23.Ad

I. INTRODUCTION

Modern experiments can fabricate semiconductor devices so small that the electron motion is two dimensional (2D) and the electron mean free path is larger than the device size. The electron transport in these devices has been of great interest both theoretically¹ and experimentally for several years. Studies of magnetotransport have led to fundamental advances such as the discovery of the quantum Hall effect,² to applied devices such as magnetic field sensors, and spin-based devices.³

Recent experiments in InSb four-terminal devices⁴ have observed a significant bend resistance, R_B . In bend-resistance experiments (Fig. 1), a current I_{14} is injected in lead 4 and removed from lead 1. If the electrons travel ballistically, they will overshoot lead 1 and travel to lead 3 until sufficient charge accumulates to deflect current to lead 4. This produces a negative voltage between leads 2 and 3. The ratio between this voltage V_{23} and I_{14} defines the bend resistance $R_B \equiv V_{23}/I_{14}$, which is also negative. When a magnetic field B is applied perpendicular to the device, charge is deflected into lead 2 decreasing V_{23} . The bend resistance therefore decreases as a function of the applied magnetic field.

Similar experiments on GaAs devices have been explained using a semiclassical billiard ball model.⁵ However the effective mass in InSb is very small ($m^* = 0.0139m_0$), and experimental features may contain few transverse quantum states below the Fermi energy. InSb devices also display ballistic transport at relatively high temperatures.⁷ Thus it is more reasonable to model this experiment using quantum mechanics and the Landauer-Buttiker formula.⁸ The Landauer-Buttiker (LB) formula states that the transport properties of a quantum-mechanical device can be obtained from the transmission coefficients of charge carriers in the device. In particular, the bend resistance can be obtained by^{6,9,10}

$$R_B = \frac{h}{2e^2} \frac{T_{41}T_{21} - T_{31}^2}{S}, \quad (1)$$

where S is given by

$$S = (T_{21} + T_{41})[(T_{21} + T_{31})^2 + (T_{41} + T_{31})^2]. \quad (2)$$

In the above equations, T_{ij} is the transmission coefficient of electrons in the lead i when the electron is injected from the

lead j . Therefore we need to calculate the transmission coefficients of electrons in the device if we want to analyze the device quantum mechanically.

A technique like a Green's-function method can calculate the transmission coefficients of electrons in a device with a simpler geometry, however when the geometry becomes complicated, it is hard to use such techniques.

In this article, we discuss R -matrix theory, a method to calculate the transmission coefficients of electrons in a device with a complicated geometry. R -matrix theory (RMT) was originated in studies of nuclear reactions in which the scattering regions have a spherical geometry.¹¹ Elsewhere,¹² we discuss the extension of RMT for two-dimensional devices. Here we present the extension of RMT to calculate the transmission coefficients of a two-dimensional device in the presence of an external perpendicular magnetic field. Even though the device made by Goel *et al.* has a complicated geometry, we focus only on a four-terminal “cross”-junction device in order to develop the general formalism of device R -matrix theory in an external magnetic field.

In Sec. II below we set up the problem to be solved and define our notation. We then discuss the problem in three steps: we first construct the lead solutions (Sec. II A), then the interior region solutions (Sec. II B) and in Sec. II C we put these two solutions together to formulate the equations,

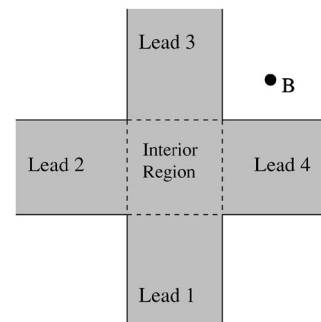


FIG. 1. A schematic of a device used in a negative bend-resistance experiment. The current is injected from lead 4 and removed from lead 1. This produces a voltage between the leads 2 and 3, V_{23} , that is measured as a function of the applied perpendicular magnetic field B . The dotted lines indicate “soft boundaries,” mathematical surfaces that serve to separate the interior region from the leads in order to facilitate the solution.

which can be solved for the transmission coefficients of electrons in the leads. As an application, in Sec. III A, we use the magnetic-field RMT to calculate the transmission coefficients in a two-dimensional four-terminal ‘‘cross’’-junction device (Fig. 1) and in Sec. III B we use these transmission coefficients to calculate the magnetotransport properties of the device. We conclude with a summary. The appendix reviews standard R -matrix theory for the field-free case.

II. SETTING UP THE PROBLEM

In order to calculate the magnetotransport properties of the electrons in the device (Fig. 1), we need to calculate the transmission coefficients of electrons in the device. In this model, we assume that the electron transport is ballistic and we model the transport by a single-electron picture. We start with the time-independent Schrodinger equation for an electron in an applied perpendicular magnetic field,

$$\hat{\mathcal{H}}|\Psi_{E,p_0,n_{p_0}}\rangle = E|\Psi_{E,p_0,n_{p_0}}\rangle, \quad (3)$$

where $|\Psi_{E,p_0,n_{p_0}}\rangle$ is the scattering wave function. The subscript E is the total energy and n_{p_0} denotes the quantum number of the incoming electron in the lead p_0 ; no other incoming channel is occupied. The Hamiltonian $\hat{\mathcal{H}}$ is given by

$$\hat{\mathcal{H}} = \frac{1}{2m^*}(\vec{P} - e\vec{A})^2 + V(\vec{r}), \quad (4)$$

where \vec{A} is the vector potential. We have chosen $V(\vec{r})=0$ inside the device, although this is not essential to the R -matrix formalism.

We will first make the Hamiltonian dimensionless. We measure the lengths in terms of a characteristic length in the device (typically we choose w_{p_0} , the width of the input lead), and energies in terms of $E_0 = \hbar^2/m^*w_{p_0}^2$ and define $\epsilon = E/E_0$ and $l_B^2 = \hbar/eB$. This new quantity l_B has the units of length and is called the ‘‘magnetic length.’’ It is the average radius of the lowest Landau level of the system. Finally, we define the dimensionless magnetic field, $\mathcal{B} = w_{p_0}^2/l_B^2$ so that the Schrodinger equation becomes

$$\left[-\frac{1}{2} \left(\frac{\partial^2}{\partial x^2} + \frac{\partial^2}{\partial y^2} \right) + i\mathcal{B} \left(\mathcal{A}_x \frac{\partial}{\partial x} + \mathcal{A}_y \frac{\partial}{\partial y} \right) + \frac{\mathcal{B}^2}{2} (\mathcal{A}_x^2 + \mathcal{A}_y^2) \right] \times |\Psi_{\epsilon,p_0,n_{p_0}}\rangle = \epsilon |\Psi_{\epsilon,p_0,n_{p_0}}\rangle, \quad (5)$$

where x and y are the dimensionless coordinates and \vec{A} is the dimensionless vector potential. In the symmetric gauge, we have $\vec{A}^{\text{symm}} = (-y/2, x/2, 0)$ and in the asymmetric gauge, $\vec{A}^{\text{asymm}} = (-y, 0, 0)$. While both gauges produce the same magnetic field, the choice of gauge is important when we solve the problem approximately. We have to choose the gauge such that the solution will satisfy the boundary conditions of the system. An appropriate choice of gauge will achieve faster convergence of the results. Since the eigenstates in any gauge form a complete basis set, we are free to

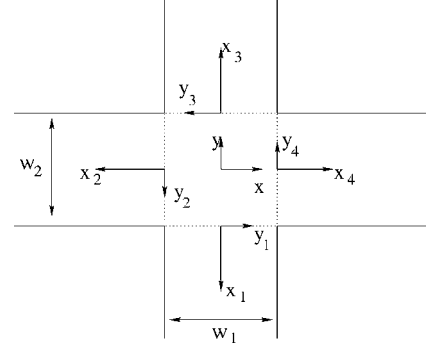


FIG. 2. A detailed schematic diagram of a four-terminal ‘‘cross’’-junction device. A local coordinate system is defined to each lead (x_q, y_q) and the interior region (x, y) . For each lead, x_q is the longitudinal coordinate and y_q is the transverse coordinate. We set the lead coordinate systems such that $x_q=0$ where lead meets the interior region.

choose whichever basis set is more convenient when expanding the final scattering wave function. We do not examine multiply connected structures and thus do not enforce any global phase relationships.

We use R -matrix theory to solve this equation for a given system. The idea of R -matrix theory is to solve for the coefficients of electrons without solving for the total scattering-wave function $|\Psi_{\epsilon,p_0,n_{p_0}}\rangle$. We first divide the system into two parts: the interior scattering region, and the exterior leads (see Fig. 1) and solve the Schrodinger equation in each region. Next, we match the solutions in the two types of regions on the soft boundaries, S (where the interior region meets the leads) to solve for the transmission coefficients using the R matrix.

A. Lead solutions

In the present application, we assume that the leads have a Cartesian symmetry and we use the same notation as in zero-field RMT (Appendix). In the absence of a magnetic field, the lead eigenfunctions take the form of sine functions with a wave vector proportional to $(\epsilon - \epsilon_{p,n_p})^{1/2}$ where ϵ is the total energy, ϵ_{p,n_p} is the subband energy of the n_p th quantum channel of the p th lead. However, the applied magnetic field breaks the reflection symmetry and the eigenfunctions are no longer sine functions.

We define in each lead a coordinate system (x_p, y_p) where y_p is the transverse and x_p is the longitudinal (positive, outgoing) coordinate (Fig. 2). For that coordinate system we write the gauge in asymmetric form, since this admits solutions in the form of a traveling wave in the longitudinal direction.¹³ Although the lead eigenfunctions are still analytic for a nonzero magnetic field these forms involve special functions that complicate the calculation. Therefore we seek a numeric solution for them.¹⁴

We seek a solution of the form

$$\zeta_{n_p}^p(x_p, y_p) = e^{ik_{p,n_p}x_p} f_{p,n_p}(y_p). \quad (6)$$

Tamura and Ando show¹⁴ how to calculate the expansion coefficients C_{n_p, m_p}^p such that,

$$f_{p,n_p}(y_p) = \sum_{m_p}^{\infty} C_{n_p, m_p}^p \chi_{p, m_p}(y_p), \quad (7)$$

where $\chi_{p, m_p}(y_p)$ are the transverse wave function of electrons in the lead when there is no magnetic field. This gives two sets of solutions for Eq. (6); half are left moving and half are right moving. The wave vector, k_{p, n_p} [Eq. (6)] can be real, imaginary, or complex. The real wave vectors correspond to current-carrying waves, whereas the complex and imaginary wave vectors produce evanescent waves. While only the current-carrying waves have a physical meaning, we need to include the evanescent waves for the mathematical completeness.

It is important to note that these lead eigenfunctions are not orthogonal to each other. However they do make a complete set so that we can use them to expand the scattering-wave function in the p th lead as

$$\Psi_{\epsilon, p_0, n_{p_0}}(x_p, y_p) = \sum_{n_p}^N \tau_{n_p, n_{p_0}}^{p, p_0} e^{ik_{p, n_p} x_p} f_{p, n_p}(y_p). \quad (8)$$

The expansion coefficients $\tau_{n_p, n_{p_0}}^{p, p_0}$ are the transmission amplitudes of interest. In particular, $\tau_{n_p, n_{p_0}}^{p, p_0}$ is the transmission amplitude of the electron to the n_p th subband in the p th lead when the electron is injected from the n_{p_0} th subband in the p_0 th lead. We use these transmission amplitudes to calculate the transmission coefficients we describe as follows.

The flux in each outgoing lead can be calculated as¹⁵

$$J_p \sim \int \left[\Psi_{\epsilon, p_0, n_{p_0}}^*(\mathbf{r}_p) \left(-i \frac{d}{dx_p} - A_x \right) \Psi_{\epsilon, p_0, n_{p_0}}(\mathbf{r}_p) + \Psi_{\epsilon, p_0, n_{p_0}}(\mathbf{r}_p) \left(i \frac{d}{dx_p} - A_x \right) \Psi_{\epsilon, p_0, n_{p_0}}^*(\mathbf{r}_p) \right] dy_p, \quad (9)$$

where $\mathbf{r}_p = (x_p, y_p)$. Since we have not normalized the eigenfunctions to unit flux, the flux in the p th lead is not given by $\sum_{n_p} |\tau_{n_p, n_{p_0}}^{p, p_0}|^2$. Once we solve for the $\tau_{n_p, n_{p_0}}^{p, p_0}$ s we can calculate the current going through each lead in the device according to Eq. (9). Even though we use N subbands in the expansion of Eq. (8), not all of them are current carrying. We determine the value of N such that the calculation gives the desired precision. This number is always larger than the number of open channels at that energy. However, we use only the open channels to calculate the flux going through the lead according to Eq. (9). The transmission coefficients from lead q to lead p are then equal to J_p/J_q .

In order to calculate the flux, we substitute Eq. (8) in Eq. (9). One might conclude that due to the nonorthogonality of the lead eigenfunctions, the cross terms will not cancel out and we will end up having a position-dependent flux, which would be puzzling. This problem does not arise however, since two lead eigenfunctions of the same energy satisfy¹⁵

$$\int_{-w_p/2}^{w_p/2} dy_p f_{k_{p, v_p}}(y_p) f_{k_{p, \beta_p}}(y_p) (k_{p, v_p} + k_{p, \beta_p} + 2y_p \mathcal{B}) = 0. \quad (10)$$

Even though the lead eigenfunctions do not obey the standard orthogonality relation, this relation [Eq. (10)] will cancel out the cross terms in the flux calculation.

B. Interior region solution

As Bloch first pointed out,¹⁶ the kinetic-energy term in a Hamiltonian in general is not Hermitian in a finite region (e.g., our interior region) for arbitrary boundary conditions. If it is not Hermitian, its eigenfunctions do not make a complete set. He defined the ‘‘Bloch Hamiltonian’’ of a system, adding a term \mathcal{L} to the original Hamiltonian so that the result is Hermitian in the finite interior region. The scattering-wave function in the interior region can then be expanded in terms of the Bloch eigenfunctions (see Appendix).

First we find the Bloch Hamiltonian corresponding to the magnetic Hamiltonian [Eq. (4)]. The form of the Hamiltonian depends on the gauge, so the Bloch term also will be gauge dependent. We will first discuss the problem for an arbitrary gauge and then give the form of the Bloch operator for the symmetric and asymmetric gauges. In the presence of a magnetic field, the Bloch operator takes the form

$$\hat{\mathcal{H}}_B = \hat{\mathcal{H}}_0 + \mathcal{H}_{\text{mag}} + \hat{\mathcal{L}}_1 + \hat{\mathcal{L}}_2. \quad (11)$$

$\hat{\mathcal{H}}_0$ is the magnetic-field independent (i.e., $\mathcal{B}=0$) part of the Hamiltonian and \mathcal{L}_1 is the magnetic-field independent Bloch operator (Appendix) in traditional R -matrix theory. The magnetic-field dependent part of the Hamiltonian, \mathcal{H}_{mag} , is given by

$$\mathcal{H}_{\text{mag}} = i\mathcal{B}A_x \frac{\partial}{\partial x} + i\mathcal{B}A_y \frac{\partial}{\partial y} + \frac{\mathcal{B}^2}{2} (A_x^2 + A_y^2). \quad (12)$$

In order to make this Hermitian we must add to it a second Bloch operator \mathcal{L}_2 , which we now derive.

The third term in Eq. (12) is just a multiplicative term that is Hermitian independent of the gauge, thus there is no contribution to the Bloch operator from the third term. We have to consider the Hermiticity of the first two terms. We will consider the first term,

$$\hat{h} = i\mathcal{B}A_x \frac{\partial}{\partial x}. \quad (13)$$

We add a term \mathcal{L}_2^x to \hat{h} such that the operator $\hat{h} + \mathcal{L}_2^x$ is Hermitian. In order to have the Hermiticity, two eigenfunctions of the operator $\hat{h} + \mathcal{L}_2^x$, f and g , should satisfy the relation

$$\langle f | (\hat{h} + \hat{\mathcal{L}}_2^x) g \rangle = \langle (\hat{h} + \hat{\mathcal{L}}_2^x) f | g \rangle. \quad (14)$$

In order to satisfy the relation we find

$$\hat{\mathcal{L}}_2^x = - \sum_{s_p} \frac{i\eta\mathcal{B}}{2} \delta(x - s_p) A_x, \quad (15)$$

where η is positive for the upper integration boundaries and negative for the lower integration boundaries. Essentially, η

is the dot product of the outward-going normal to the soft boundary and the direction of the gradient. Note that the Bloch operator has a different form compared to the zero-field Bloch term. In the zero-field expression the Bloch term is equal to the boundary term, whereas in the magnetic-field problem, the Bloch-operator term is the half of the boundary term.

In the same way, we can make the y -dependent part of the Hamiltonian Hermitian and we get the total magnetic Bloch term as

$$\hat{\mathcal{L}}_2 = - \sum_{s_p^x} \frac{i\eta\mathcal{B}}{2} \delta(x - s_p^x) \mathcal{A}_x - \sum_{s_p^y} \frac{i\eta\mathcal{B}}{2} \delta(y - s_p^y) \mathcal{A}_y, \quad (16)$$

where the first term runs over all the x boundaries and the second term runs over all the y boundaries. When solving for the interior region eigenfunctions, we use the symmetric gauge and the magnetic Bloch term takes the form

$$\mathcal{L}_2^{\text{sym}} = \sum_{s_p^x} \frac{i\eta\mathcal{B}}{4} \delta(x - s_p^x) y - \sum_{s_p^y} \frac{i\eta\mathcal{B}}{4} \delta(y - s_p^y) x. \quad (17)$$

When solving for the lead eigenfunctions, we use the asymmetric gauge and the magnetic Bloch term takes the form

$$\mathcal{L}_2^{\text{asym}} = \sum_{s_p^x} \frac{i\eta\mathcal{B}}{2} \delta(x - s_p^x) y. \quad (18)$$

The two Bloch terms $\mathcal{L}_1 + \mathcal{L}_2$ make \mathcal{H}_B Hermitian and we use its eigenfunctions ϕ_j to expand the scattering wave functions in the interior region as

$$|\Psi_\epsilon\rangle = \sum_j \mathcal{C}_j |\phi_j\rangle. \quad (19)$$

In the following section we explain how to relate the interior region solution [Eq. (19)] and the lead solution [Eq. (8)] to solve for the transmission amplitudes $\tau_{n_p, n_{p_0}}^{p, p_0}$.

C. R-matrix formulation

Knowing the lead eigenfunctions and the interior-region Bloch eigenfunctions, R -matrix theory allows us to formulate an equation to solve for the unknown scattering amplitudes in Eq. (8). Following the zero-field formulation in the Appendix, we note that our scattering-wave function satisfies Eq. (3) in all space while our interior Bloch eigenfunctions satisfy

$$(\hat{\mathcal{H}} + \hat{\mathcal{L}}_1 + \hat{\mathcal{L}}_2) \phi_j = \epsilon_j \phi_j.$$

Thus, within the interior region and on its boundaries we can expand the scattering-wave function in terms of the interior eigenstates. A small amount of algebra then shows that we can write the scattering-wave function in the q th lead as

$$|\Psi_{\epsilon, p_0, n_{p_0}}(x_q, y_q)\rangle = R_\epsilon(x_q, y_q; x_p, y_p) \hat{\mathcal{L}} |\Psi_{\epsilon, p_0, n_{p_0}}(x_p, y_p)\rangle, \quad (20)$$

where the R matrix is defined in Eq. (A7). In the presence of a magnetic field the Bloch operator has two terms that \mathcal{L}

$= \mathcal{L}_1 + \mathcal{L}_2$. This Eq. (20) is true only inside the interior region and we use that to write the scattering wave function on the soft boundaries where the scattering-wave function can also be expanded in terms of the lead eigenfunctions. The notation and the procedure remain the same as in the zero-field RMT, however, extra care has to be taken since the transverse lead eigenfunctions $f_{p, n_p}(y_p)$ are not orthogonal.

In Eq. (20) the Bloch eigenfunctions ϕ_j are eigenfunctions of the Bloch Hamiltonian with the symmetric gauge (since we have chosen the symmetric gauge for the interior region). However the Bloch operator appears in the right-hand side of Eq. (20) is $\mathcal{L} = \mathcal{L}_1 + \mathcal{L}_2^{\text{asym}}$, as we have chosen the asymmetric gauge for each lead.

Now the scattering-wave function in the interior region relates to the \mathcal{M} matrix as

$$|\Psi_{\epsilon, p_0, n_{p_0}}(x_q, y_q)\rangle = \sum_{n_q} \sum_p \sum_{n_p} \mathcal{M}_\epsilon(q, n_q; p, n_p) |\chi_{q, n_q}(y_q)\rangle \times \langle \chi_{p, n_p}(y_p) | (\nabla_{x_p} + i\mathcal{B}y_p) | \Psi_{\epsilon, p_0, n_{p_0}}(x_p, y_p)\rangle, \quad (21)$$

where the \mathcal{M} matrix is defined in Eq. (A10) and the index p runs through all the soft boundaries. Since we consider this equation on the soft boundaries ($x_q=0$), the scattering wave function can be written as,

$$|\Psi_{\epsilon, p_0, n_{p_0}}(x_q, y_q)\rangle = \sum_{m_q=1}^{M_q} C_{n_q, m_q}^q |\chi_{q, m_q}(y_q)\rangle \delta_{q, p_0} e^{-ik_{q, n_q} x_q} \delta_{n_q, n_{p_0}} + \sum_{n_q=1}^{N_q} \sum_{m_q=1}^{M_q} C_{n_q, m_q}^q e^{ik_{q, n_q} x_q} |\chi_{q, m_q}(y_q)\rangle \tau_{n_q, n_{p_0}}^{q, p_0}. \quad (22)$$

Combining Eqs. (21) and (22) gives a set of linear equations as

$$C_{n_q, m_q}^q \delta_{q, p_0} \delta_{n_q, n_{p_0}} + \sum_{n_q} C_{n_q, m_q}^q \tau_{n_q, n_{p_0}}^{q, p_0} = \sum_{m_p} \sum_{m'_p} \mathcal{K}_1 C_{n_{p_0}, m'_p}^p + \sum_p \sum_{m_p} \sum_{n_p} \sum_{m'_p} \mathcal{K}_2 C_{n_p, m'_p}^p \tau_{n_p, n_{p_0}}^{p, p_0}, \quad (23)$$

where \mathcal{K}_1 and \mathcal{K}_2 are defined as

$$\mathcal{K}_1 = \mathcal{M}_\epsilon(q, m_q, p_0, m_p) (i\mathcal{B} \langle y_{m_p, m'_p} \rangle - ik_{p_0, n_{p_0}} \delta_{m_p, m'_p}), \quad (24)$$

and

$$\mathcal{K}_2 = \mathcal{M}_\epsilon(q, m_q, p, m'_p) (i\mathcal{B} \langle y_{m_p, m'_p} \rangle + ik_{p, n_p} \delta_{m_p, m'_p}).$$

In the above equations,

$$\langle y_{m_p, m'_p} \rangle = \langle \chi_{p, m_p} | y_p | \chi_{p, m'_p} \rangle. \quad (25)$$

Note the difference between Eq. (A9) and Eq. (23). The extra complexity in the magnetic-field RMT is due to the nonorthogonality of the lead eigenfunctions and the additional term in the Bloch operator. This equation [Eq. (23)] can be solved for the unknown transmission amplitudes, $\tau_{n_q, n_{p_0}}^{q, p_0}$. We will calculate the \mathcal{M} matrix elements using a variational ba-

sis set. In order to explain the procedure, we will calculate the scattering coefficients of a four-terminal ‘‘cross’’ junction.

III. APPLICATIONS: FOUR-TERMINAL ‘‘CROSS’’ JUNCTION

A. Transmission coefficients

In this section we show how to apply Eq. (23) to calculate the transmission coefficients for the electrons injected into the device shown in Fig. 1. In order to ease the explanation, we draw a detailed diagram of the device as shown in Fig. 2. This device has a symmetric geometry in that all the leads are the same in width. However, the technique does not require such a symmetry in the device.

In order to calculate the transmission coefficients of the electrons in this system, we need to simultaneously solve the set of equations given by Eq. (23), which requires the matrix elements of \mathcal{M} . The \mathcal{M} matrix elements are defined by the interior-region eigenfunctions $|\phi_j\rangle$ [Eq. (A10)]. We use a variational basis set to calculate those interior region eigenfunctions. We briefly explain the variational approach below.¹⁷

The interior region eigenfunctions are solutions to the equation

$$\mathcal{H}_B|\phi_j\rangle = \epsilon_j|\phi_j\rangle. \quad (26)$$

We choose the symmetric gauge for the interior region for which the field-dependent Bloch-Hamiltonian term takes the form

$$\begin{aligned} \mathcal{L}_2 = & -\frac{iy\mathcal{B}}{4}\delta\left(x + \frac{w_1}{2}\right) + \frac{iy\mathcal{B}}{4}\delta\left(x - \frac{w_1}{2}\right) + \frac{ix\mathcal{B}}{4}\delta\left(y + \frac{w_2}{2}\right) \\ & - \frac{ix\mathcal{B}}{4}\delta\left(y - \frac{w_2}{2}\right). \end{aligned} \quad (27)$$

We use a set of basis functions

$$\begin{aligned} |\eta_a(x)\rangle &= \sqrt{\frac{1}{\lambda_x}} = \sqrt{\frac{2}{\lambda_x}} \sin \frac{a\pi}{\lambda_x} x \quad \text{for } a = 1, 3, \dots \\ &= \sqrt{\frac{2}{\lambda_x}} \cos \frac{a\pi}{\lambda_x} x \quad \text{for } a = 2, 4, \dots \end{aligned}$$

for x direction and a similar set $\xi_b(y)$ for the basis functions in the y direction.

Note that, if we set $\lambda_x=1$ and $\lambda_y=1$, these basis functions make an orthonormal set, which satisfy the logarithmic derivative boundary conditions. However, we choose λ_x and λ_y slightly larger than 1 (e.g., $\lambda_x=1.3$), which makes this set nonorthonormal; it is complete inside the interior region.

The importance of using such a variational basis function is that those basis functions do not have any common boundary conditions (such as zero value or zero derivative) on the soft boundaries s_q . Having different values and different derivatives on the boundaries achieves a faster convergence in expanding the scattering-wave function $|\Psi_{\epsilon, p_0, n_{p_0}}\rangle$ since the scattering-wave function is not found to obey any particular condition on these boundaries.

Since the basis set is not orthonormal, we need to solve the generalized eigenvalue problem to calculate the eigenvalues ϵ_j and the corresponding eigenvectors $|\phi_j\rangle$ with the expansion coefficients which are defined as,

$$|\phi_{n,m}(x,y)\rangle = \sum_{a,b} d_{n,m,a,b} |\eta_a(x)\rangle |\xi_b(y)\rangle. \quad (28)$$

We calculate the \mathcal{M} matrix elements and then solve the linear algebra equations [Eq. (23)] to find the scattering amplitudes $\tau_{n_q, n_{p_0}}^{q, p_0}$. In the interior region calculation, we use 100 basis functions to diagonalize the Bloch Hamiltonian (obtained from a product of 10 basis functions in the y -direction and 10 in the x -direction). We use the same number of basis functions, ten basis functions to expand the lead eigenfunctions. This makes sure that we have enough basis functions. However, we have not optimized the code to use the least required number of evanescent functions. Once we know the scattering amplitudes $\tau_{n_q, n_{p_0}}^{q, p_0}$, we can calculate the transmission coefficients in each lead as we explained in Sec. II A.

The graph (Fig. 3) shows the transmission coefficients of the electrons in the four-terminal square-junction device for different values of magnetic fields. The plotted values are the lead to lead transmission coefficients, $T_{q p_0} = \sum_{n_q, n_{p_0}} \mathcal{T}_{n_q, n_{p_0}}^{q, p_0}$, where $\mathcal{T}_{n_q, n_{p_0}}^{q, p_0}$ is the transmission coefficient of electrons to the n_q th channel in the q th lead when the electron is injected from the n_{p_0} th channel in the p_0 th lead. We have considered an electron injected from the lead 1 so that $p_0=1$. As a check of the method, we set $\mathcal{B}=0$ and calculate the transmission coefficients [Fig. 3(a)]. The transmission coefficients for the left and right directions, T_{41} and T_{21} , are identical. That is because of the symmetry when there is no magnetic field. The results show that the magnetic-field RMT correctly recovers the zero-field result. Note that the forward transmission T_{31} is always higher than the left and right transmission when there is no magnetic field. That means, even though the current source drives electrons from lead 1 to lead 4, electrons are more likely to travel ballistically to lead 3 (the forward lead). If electrons moved diffusively, they would pile up equally in the leads 2 and 4. In contrast, ballistic electrons will accumulate in the forward lead giving a negative voltage V_{23} , which results in a negative bend resistance.

As the magnetic field is increased, electrons experience the Lorentz force and tend to deflect to the lead 2. The transmission coefficient T_{21} is higher than the transmission coefficient T_{41} as we observe from the transmission coefficients at $\mathcal{B}=6$ and $\mathcal{B}=12$ [Figs. 3(b) and 3(d)]. Also, the transmission coefficients at $\mathcal{B}=6$ and $\mathcal{B}=-6$ [Figs. 3(b) and 3(c)] show that the direction of the electron path changes as you change the direction of the magnetic field, which again demonstrates the accuracy of the calculation. Knowing the transmission amplitudes, we can calculate scattering-wave function. We have plotted the probability density of a positively charged particle traveling in the four-terminal junction at energy $\epsilon=25$. We show (Fig. 4) both the zero-field scattering-wave function and the wave function at $\mathcal{B}=10$. We can see the symmetry of the scattering wave function when there is

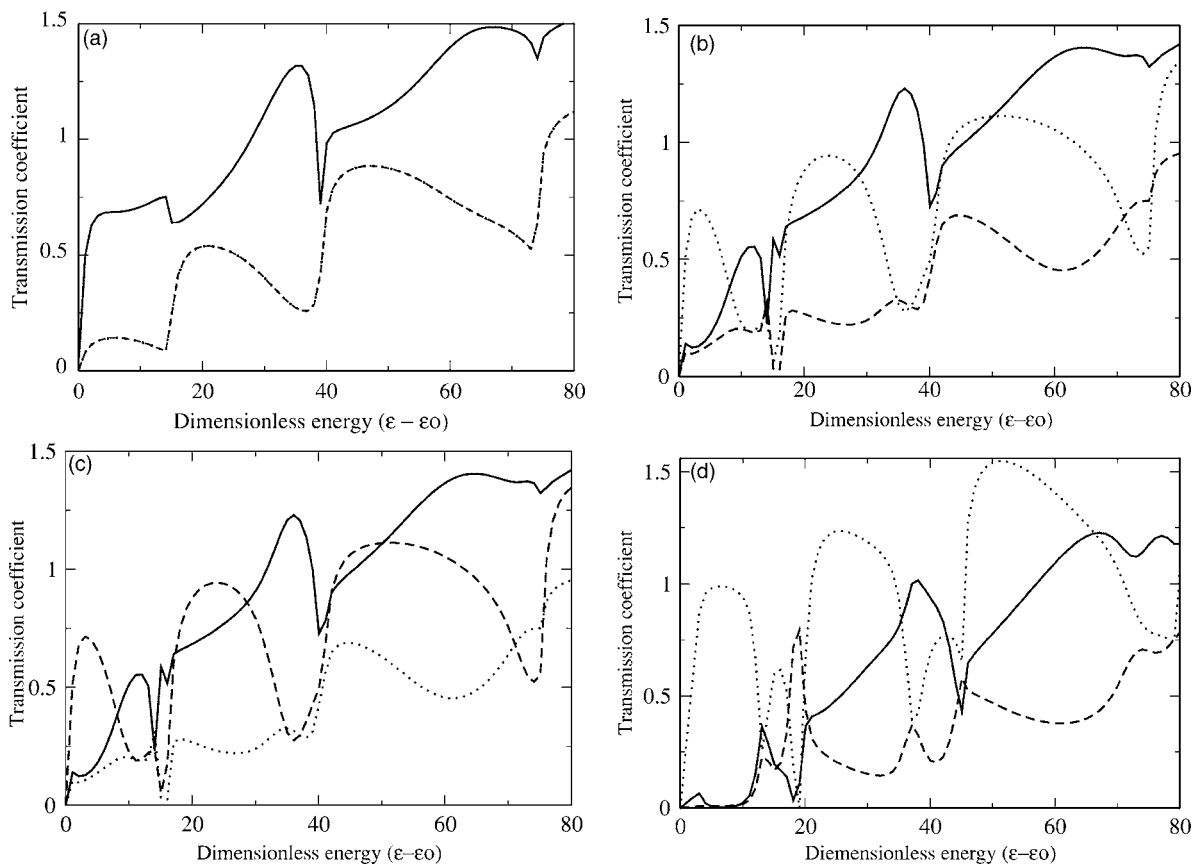


FIG. 3. Transmission coefficients for the electron injected to the four-terminal “cross” junction device (Fig. 1) for (a) $B=0$, (b) $B=6$, (c) $B=-6$, and (d) $B=12$. The solid line is T_{31} , the dotted line is T_{21} , and the dashed line is T_{41} .

no magnetic field and how the electron deflects towards the side arm when there is a magnetic field perpendicular to the system.

B. Calculating the magnetotransport properties

In the previous section we calculated the transmission coefficients of electrons injected to a four-terminal device at

different energies. Now we use these transmission coefficients to calculate the transport properties according to the LB theory. At zero temperature, only the transmission coefficients at the Fermi energy contribute to the transport properties. The Fermi energy is represented by a specific value of the dimensionless energy on the horizontal axis of graphs in Fig. 3. This dimensionless energy is measured relative to the

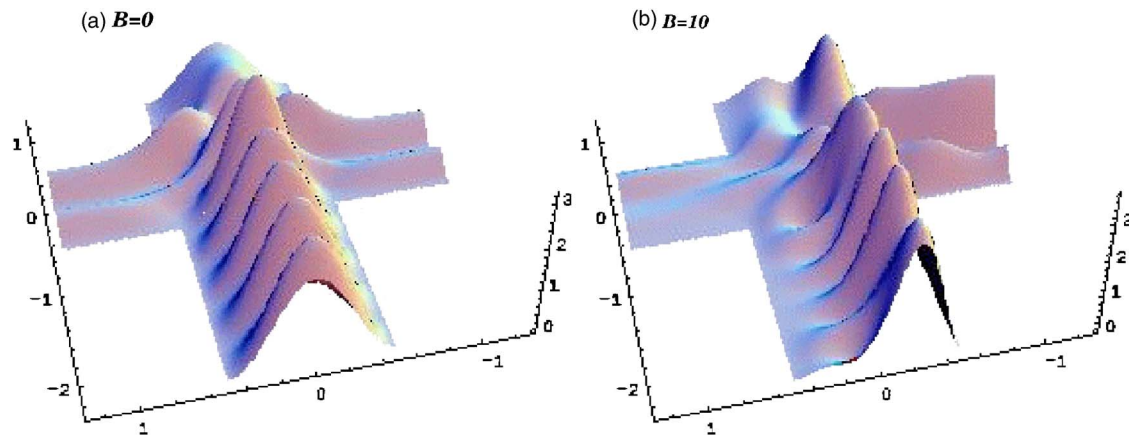


FIG. 4. (Color online) The probability density of a positively charged particle injected into the four-terminal “cross” junction. (a) is the probability density of the particle when there is no magnetic field and (b) is the probability density when the applied perpendicular magnetic field $B=w_0^2/l_B^2=10$. Both the probabilities are calculated when the scattering energy, $\epsilon=25$. Note that the sidearms have similar probabilities for the left figure, but not for the right figure.

TABLE I. Dimensionless Fermi energy values (i.e., energy measured in units of E_0) are converted into corresponding widths for a sample with the electron concentration $n=1.90 \times 10^{11} \text{ cm}^{-2}$.

Dimensionless Fermi energy	Width (nm)
30	71
35	76
40	82
50	91
60	100

ground-state energy of the input lead, i.e., $(\epsilon - \epsilon_0)$ where $\epsilon = E/E_0$ and $\epsilon_0 = \pi^2/2$, ground-state energy in the input lead in the dimensionless units. Since the energy unit E_0 depends on the width of the input lead w_{p_0} , for a given Fermi energy, the energies at different points on the horizontal axis represent devices with different widths w_{p_0} . The Fermi energy of a system is set by the electron concentration, n , of the system so that

$$E_F = \frac{\pi \hbar^2}{m^*} n, \quad (29)$$

where m^* is the effective mass of electrons in the device. Therefore, we can convert the values of the dimensionless energy in the transmission coefficient graphs to the device width according to

$$\epsilon_F \frac{\hbar^2}{m^* w_{p_0}^2} = \frac{\pi \hbar^2}{m^*} n, \quad (30)$$

where ϵ_F is the Fermi energy in dimensionless units. Given the electron concentration of the sample, we can convert the dimensionless Fermi energy ϵ_F into the width of the device as

$$w_{p_0} = \sqrt{\frac{\epsilon_F}{\pi n}}. \quad (31)$$

Table I shows the conversion of the Fermi energies that we have considered in the R_B calculation (Fig. 5) to the width of the device for an electron concentration $n=1.90 \times 10^{11} \text{ cm}^{-2}$.

Knowing the transmission coefficients at the Fermi energy, we calculate the bend resistance R_B according to Eq. (1) at different intensities of the external magnetic field. Also note that, in the calculation, we measure the magnetic field in dimensionless units, $\mathcal{B} = w_{p_0}^2 / l_B^2$. For a given w_{p_0} , we can convert the units of the magnetic field to Tesla according to this relation. We calculate the R_B at different dimensionless Fermi energies (for devices with different widths) and the result is shown in Fig. 5. The Fermi energy decreases means the width of the device decreases as shown in the Table I.

Our calculations show that the bend resistance is negative at zero magnetic field, which qualitatively agrees with the experimental observation made by Goel *et al.*,⁴ and the width of the peak is comparable to experiment. However, the de-

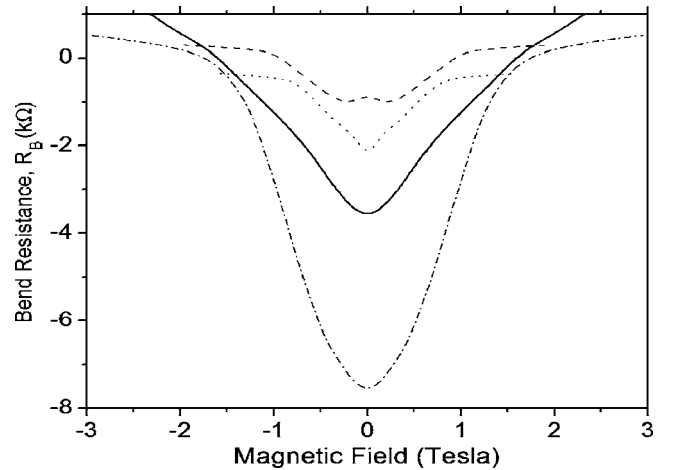


FIG. 5. The bend resistance R_B of a four-terminal “cross”-junction device as calculated using the magnetic field R -matrix theory and LB formula. We have calculated the bend resistance at different Fermi energies ϵ_F equal to 30 (solid), 35 (dashed), 40 (dotted), 50 (short dashed), and 60 (dashed-dotted). These different lines correspond to different device sizes as shown in Table I.

tails of their device geometry is sufficiently different from ours that it is hard to compare the results quantitatively. Our calculations also show that the variation of the bend resistance with magnetic field is not monotonic with the width of the sample. In order to clarify this point, we plot the bend resistance R_B as a function of sample width in Fig. 6.

The bend resistance depends on ratios of transmission coefficients at the Fermi energy, and the graphs of Fig. 3 show that these ratios do not have a simple dependence on energy. In particular, the transmission coefficients vary rapidly as we pass through a threshold. If the width of the sample is such that the Fermi energy lies close to a threshold energy, then the difference between T_{31} and T_{21} is large and we will get a large negative bend resistance. However, if the Fermi energy lies away from a threshold energy, this difference decreases, lowering the R_B . It is not just the width of the sample matters

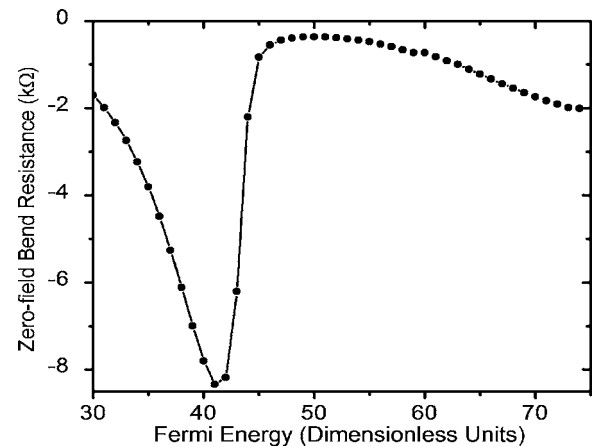


FIG. 6. The bend resistance R_B of a four-terminal “cross”-junction device is calculated at $\mathcal{B}=0$ for different values of Fermi energies, i.e., different device sizes for a given electron concentration.

for the result, but the position of the Fermi energy with respect to the threshold energies. These issues have yet to be explored by experiment.

Experiments⁴ have reported $R_B \sim 5 \text{ k}\Omega$ when the width of the sample is equal to $0.2 \text{ }\mu\text{m}$. According to our results, this high bend resistance can be seen only for a narrower device. However, the reported width is the lithographic width, and the actual channel width can be much lower due to depletion. This is supported by the fact that many devices were found to be close to the threshold of pinchoff.

IV. DISCUSSION AND CONCLUSION

It is useful to contrast our quantum-mechanical results with a semiclassical diffusive model. Since the actual width of a quantum wire can easily be much smaller than its lithographic width, it can be unclear whether or not a device is dominated by quantum-mechanical effects. Hallmarks of the quantum approach include: nonmonotonic dependence of the bend resistance on the device width (or Fermi energy), extreme sensitivity to device geometry, and damped oscillations in the bend resistance as a function of magnetic field. Diffusive models,⁵ by contrast, give monotonic behavior as a function of device width, general insensitivity to minor changes in device geometry, and a nonoscillatory behavior in the bend resistance as a function of magnetic field.

Experiments in semiconductor systems that are well in the semiclassical limit display a smooth dependence on device size.⁵ Recent experiments by Goel *et al.*,⁴ which are closer to the quantum-mechanical limit, display damped oscillations in the bend resistance as a function of field. As device sizes shrink, the quantum approach may be more relevant, especially in systems with a small effective mass.

In conclusion, we have improved upon the existing zero-field R -matrix theory to calculate the transmission coefficients of electrons in two-dimensional device in the presence of an external magnetic field. Using the magnetic field RMT, we show how to calculate the magnetotransport properties of a four-terminal device in a fully quantum-mechanical fashion.

R -matrix theory provides a fast way to analyze these devices. However, its true advantage comes in analyzing many-electron systems. Future work will involve applying the formalism to calculating the magnetoresistance of molecular wire systems.

ACKNOWLEDGMENTS

We wish to thank Michael Santos for many useful discussions, as well as Niti Goel. This project was supported in part by U.S. National Science Foundation under Grants No. MR-SEC DMR-0080054, and No.EPS-9720651. One of the authors (T. J.) would like to acknowledge the University of Oklahoma Graduate College for travel and research grants.

APPENDIX: ZERO-FIELD R -MATRIX THEORY FOR A 2D SYSTEM

We consider the two-dimensional system in Fig. 7. This system has a central region A connected to N external re-

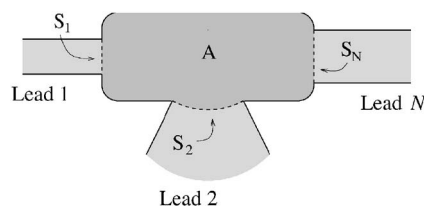


FIG. 7. Schematic of a two-dimensional device for the present scattering calculations. The mathematical surfaces s_1, s_2, \dots, s_N separate the interior region A from the N leads, but do not correspond to physical interfaces.

gions or “leads.” The leads and the interior region meet at a set of boundary mathematical surfaces we denote by s_1, s_2, \dots, s_N . We treat the boundaries between the shaded and unshaded regions as “hard walls” (infinite potential) so electron wave functions are nonzero only in the shaded regions. The surfaces, s_1, s_2, \dots, s_N are called the “soft boundaries.” We denote the input lead by p_0 and all other leads by positive integer p . We measure all distances in units of w_{p_0} and energies in terms of $E_0 \equiv \hbar^2/m^*w_{p_0}^2$. We seek an analytic solution for the amplitudes of outgoing states in the leads when only one incoming state is occupied.

The time-independent Schrödinger equation for the scattering function is

$$(\hat{H} - \epsilon)|\Psi_{\epsilon, p_0, n_{p_0}}\rangle = 0, \quad (\text{A1})$$

where $|\Psi_{\epsilon, p_0, n_{p_0}}\rangle$ represents the state of an electron with total energy ϵ incident in input-lead subband n_{p_0} . Note that $|\Psi_{E, p_0, n_{p_0}}\rangle$ is well defined in all leads. In a *finite* region, the Hamiltonian \hat{H} is not Hermitian. We can, in general, produce a Hermitian operator by adding to \hat{H} the so-called Bloch operator $\hat{\mathcal{L}}_1$.¹⁸ Usually in zero-field RMT, we use \mathcal{L}_B for the Bloch operator, however we save the symbol B for the magnetic field in this paper. We denote the eigenfunctions of the sum of these operators in the interior region by $|\phi_j\rangle$ and write the so-called Bloch eigenvalue equation as

$$(\hat{H} + \hat{\mathcal{L}}_1)|\phi_j\rangle = \epsilon_j|\phi_j\rangle. \quad (\text{A2})$$

Inserting the Bloch operator into the Schrödinger equation we get

$$(\hat{H} + \hat{\mathcal{L}}_1 - \epsilon)|\Psi_{\epsilon, p_0, n_{p_0}}\rangle = \hat{\mathcal{L}}_1|\Psi_{\epsilon, p_0, n_{p_0}}\rangle. \quad (\text{A3})$$

For a free-particle system, the Bloch operator takes the form

$$\mathcal{L}_1 = \sum_p \frac{1}{2} \delta(x - s_p) \vec{\nabla} \cdot \hat{n}, \quad (\text{A4})$$

where \hat{n} is the perpendicular norm to the boundary. We now expand the scattering-wave function $|\Psi_{\epsilon, p_0, n_{p_0}}\rangle$ in the set of orthonormal Bloch eigenfunctions

$$|\Psi_{\epsilon, p_0, n_{p_0}}\rangle = \sum_j C_j |\phi_j\rangle. \quad (\text{A5})$$

Inserting this expansion into the Schrödinger equation and using the properties of the Bloch eigenfunctions, we can write the scattering function on the q th lead as

$$|\Psi_{\epsilon, p_0, n_{p_0}}(x_q, y_q)\rangle = R_{\epsilon}(x_q, y_q; x_p, y_p) \mathcal{L}_1 |\Psi_{\epsilon, p_0, n_{p_0}}\rangle, \quad (\text{A6})$$

where

$$R_{\epsilon}(x_q, y_q; x_p, y_p) = \sum_j \frac{|\phi_j(x_q, y_q)\rangle \langle \phi_j(x_p, y_p)|}{\epsilon_j - \epsilon}. \quad (\text{A7})$$

This expansion is valid throughout the interior region A and on its surface (see Fig. 7).

We now apply this expansion of the scattering state on each boundary s_q . At each such boundary we can expand the scattering function in either lead eigenfunctions or Bloch eigenfunctions in the interior region. To be specific, we introduce a local Cartesian coordinate system for each lead: x_q and y_q , the longitudinal and transverse coordinates of the n_q th lead, respectively. We choose $x_q=0$ on each boundary. (One can easily choose any orthonormal coordinate system, *mutatis mutandis*.) Each lead eigenfunction is then a product of a plane wave in the x_q direction and a transverse bound-state eigenfunction $|\chi_{q, n_q}(y_q)\rangle$. The scattering-wave function in the n_q th lead therefore becomes

$$\begin{aligned} |\Psi_{\epsilon, p_0, n_{p_0}}(x_p, y_p)\rangle &= e^{-ik_{p_0, n_{p_0}} x_{p_0}} \chi_{p_0, n_{p_0}}(y_{p_0}) \delta_{p, p_0} \\ &+ \sum_{q, n_q=1}^N \tau_{n_q, n_{p_0}}^{q, p_0}(\epsilon) e^{ik_{q, n_q} x_q} \chi_{q, n_q}(y_q) \delta_{p, q}, \end{aligned} \quad (\text{A8})$$

where k_{q, n_q} and $\tau_{n_q, n_{p_0}}^{q, p_0}$ are the wave vector and scattering amplitude for the channel with quantum number n_q in lead q . Finally, $\delta_{p, q}$ is the Kronecker delta function, which ensures that each wave function is defined only in one lead. We can express energy conservation in lead q as $\epsilon = k_{q, n_q}^2 + \epsilon_{q, n_q}$, where ϵ_{q, n_q} is the energy associated with the n_q th subband in the q th lead. We use this relation to determine the wave vector k_{q, n_q} .

After some algebra we get a set of linear algebraic equations that we can solve for the transmission amplitudes;

$$\begin{aligned} i \sum_{p, n_p} \tau_{n_p, n_{p_0}}^{p, p_0}(\epsilon) k_{p, n_p} M_{\epsilon}(q, n_q, p, n_p) - \tau_{n_q, n_{p_0}}^{q, p_0} \\ = \delta_{q, p_0} \delta_{n_q, n_{p_0}} + ik_{p_0, n_{p_0}} M_{\epsilon}(q, n_q, p_0, n_{p_0}). \end{aligned} \quad (\text{A9})$$

In writing these equations we have defined

$$M_{\epsilon}(q, n_q, p, n_p) = \frac{1}{2} \int_{y_p} \int_{y_q} \chi_{q, n_q}^*(y_q) R_{\epsilon}(y_q, y_p) \chi_{p, n_p}(y_p) dy_q dy_p. \quad (\text{A10})$$

Finally, the R matrix is given by

$$R(\epsilon, y_p, y_q) = \sum_j \frac{\phi_j^*(x_q=0, y_q) \phi_j(x_p=0, y_p)}{\epsilon_j - \epsilon}. \quad (\text{A11})$$

This equation is general in that we can easily adapt it to any number of leads and to different choices of input lead.

*Electronic address: thushari@ou.edu

¹O. Olendski and L. Mikhailovska, Phys. Rev. B **72**, 235314 (2005).

²F. M. Peeters, Phys. Rev. Lett. **61**, 589 (1987).

³K. J. Goldammer, S. J. Chung, W. K. Liu, M. B. Santos, J. L. Hicks, S. Raymond, and S. Q. Murphy, J. Cryst. Growth, **201/202**, 753 (1999).

⁴N. Goel, S. J. Chung, M. B. Santos, K. Suzuki, S. Miyashita, and Y. Hirayama, Physica E (Amsterdam) **21**, 761 (2004).

⁵S. Tarucha, T. Saku, Y. Hirayama, and Y. Horikoshi, Phys. Rev. B **45**, 13465 (1992).

⁶S. Datta, *Electronic Transport Properties of Mesoscopic Systems* (Cambridge University Press, Cambridge, England, 1995).

⁷Hong Chen, J. J. Heremans, J. A. Peters, N. Goel, S. J. Chung, and M. B. Santos, Appl. Phys. Lett. **84**, 5380 (2004).

⁸R. Landauer, IBM J. Res. Dev. **3**, 223 (1957).

⁹Y. Hirayama, T. Saku, S. Tarucha, and Y. Horikoshi, Appl. Phys. Lett. **58**, 2672 (1991).

¹⁰There is a factor of N (number of open channels) difference between Ref. 9 and Ref. 6 and we have used the equation from Ref. 6.

¹¹E. P. Wigner and I. Eisenbud, Phys. Rev. **72**, 29 (1947).

¹²Thushari Jayasekera, Michael A. Morrison, and Kieran Mullen (unpublished).

¹³Claude Cohen-Tannoudji, Bernard Diu, and Franck Laloe, *Quantum Mechanics* (John Wiley and Sons, New York, 1977).

¹⁴H. Tamura and T. Ando, Phys. Rev. B **44**, 1792 (1991).

¹⁵R. L. Schult, H. W. Wyld, and D. G. Ravenhall, Phys. Rev. B **41**, 12760 (1990).

¹⁶C. Bloch, Nucl. Phys. **4**, 503 (1957).

¹⁷In the atomic physics literature this approach is referred to as using a “variational basis,” even though we are not optimizing the basis respect to λ . We preserve the terminology used in the literature.

¹⁸R. K. Nesbet, S. Mazevet, and M. A. Morrison, Phys. Rev. A **64**, 034702 (2001).